ISSN 1070-3632, Russian Journal of General Chemistry, 2019, Vol. 89, No. 7, pp. 1415–1423. © Pleiades Publishing, Ltd., 2019.
Russian Text © The Author(s), 2019, published in Zhurnal Obshchei Khimii, 2019, Vol. 89, No. 7, pp. 1058–1068.

Synthesis, Structure, and Biological Activity of Coordination Compounds of Cobalt(II), Nickel(II), and Copper(II) with *N*-(Methoxyphenyl)-2-[(5-nitrofuryl)methylene]hydrazine Carbothioamides

A. P. Gulea[a], N. L. Mitkevich[a], Yu. M. Chumakov[b,c], P. A. Petrenko[b], G. G. Balan[d], O. S. Burduniuc[d,e], and V. I. Tsapkov[a]*

[a] *State University of Moldova, ul. Mateevicha 60, Kishinev, Moldova*
**e-mail: vtsapkov@gmail.com*
[b] *Institute of Applied Physics, Kishinev, Moldova*
[c] *Gebze Institute of Technology, Cayirova, Kocaeli, Turkey*
[d] *State University of Medicine and Pharmacy "Nicolae Testemitanu," Kishinev, Moldova*
[e] *National Agency of Public Health, Kishinev, Moldova*

Received December 20, 2018; revised December 20, 2018; accepted December 30, 2018

Abstract—4-(2-Methoxyphenyl)-, 4-(3-methoxyphenyl)-, and 4-(4-methoxyphenyl)-2-[(5-nitrofuryl)methylene]-hydrazine carboxamide ($HL^{1–3}$) react with hydrates of cobalt (nickel, copper) chloride (nitrate, acetate) with the formation of the $M(HL^{1–3})_2X_2$ ($M = Co^{2+}$, Ni^{2+}, Cu^{2+}; $X = Cl^–$, $NO_3^–$) and $M(L^{1–3})_2$ ($M = Ni^{2+}$, Cu^{2+}) coordination compounds. Structure of the obtained compounds has been studied by means of X-ray diffraction analysis. Their antimicrobial and antifungal activity towards a series of *Staphylococcus aureus*, *Escherichia coli*, and yeast-like fungi standard strains has been investigated.

Keywords: cobalt(II) complexes, nickel(II) complexes, copper(II) complexes, hydrazine carbothioamides, crystal structure, antimicrobial activity, antifungal activity

DOI: 10.1134/S1070363219070119

Derivatives of hydrazine carbothioamides have been widely used in medicine as antimicrobial, antituberculous, anticancer, and antifungal drugs [1, 2]. It has been shown that many coordination compounds of *d*-elements with these ligands also exhibit selective physiological activity, the sensitivity of microorganisms to the complexes being in certain cases higher than to the pure ligands [3–5]. Therefore, synthesis and study of novel complexes of bioactive metals with such ligands is of fundamental as well as practical interest.

This study aimed to synthesize and investigate the structure as well as physico-chemical, antifungal, and antimicrobial properties of cobalt, nickel, and copper complexes with 4-(2-methoxyphenyl)-, 4-(3-methoxyphenyl)-, and 4-(4-methoxyphenyl)-2-[(5-nitrofuryl)-methylene]hydrazine carbothioamide ($HL^{1–3}$, Scheme 1).

Those thioamides were prepared via the condensation of *N*-(2-methoxyphenyl)hydrazine carbothioamide or the corresponding 3- (4-) derivative with equimolar amount of 5-nitrofuran-2-carbaldehyde in ethanol. Recrystallization of thioamides $HL^{1–3}$ from ethanol and DMF afforded the monocrystals of HL^1 and $HL^1 \cdot DMF$, respectively, the structure of which was elucidated by means of X-ray diffraction analysis.

Two crystallographically independent practically planar molecules were revealed in the structure of thio-

Scheme 1.

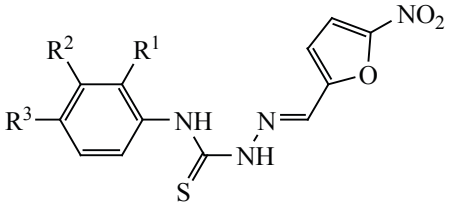

$HL^{1–3}$

$R^1 = OCH_3$, $R^2 = R^3 = H$ (HL^1); $R^1 = R^3 = H$, $R^2 = OCH_3$ (HL^2); $R^1 = R^2 = H$, $R^3 = OCH_3$ (HL^3).

Table 1. Crystallographic parameters, experimental data, and structure refinement for compounds HL^1, HL^1·DMF, and complex **8**

Parameter	HL^1	HL^1·DMF	Complex **8**
Formula	$C_{26}H_{24}N_8O_8S_2$	$C_{16}H_{19}N_5O_5S$	$C_{32}H_{36}N_{10}O_{10}S_2Ni$
M	640.65	393.42	843.54
Crystal system	Triclinic	Monoclinic	Monoclinic
Space group	*P*-1	$P2_1/c$	$P2_1/c$
Z	2	4	2
a, Å	7.0085(7)	20.7881(14)	8.1509(6)
b, Å	13.1441(14)	5.6012(4)	7.8961(6)
c, Å	17.417(2)	16.4777(13)	29.420(2)
α, deg	68.570(11)	90	90
β, deg	81.009(10)	99.655(7)	96.433(7)
γ, deg	78.204(9)	90	90
V, Å^3	1456.1(3)	1891.5(2)	1881.5(2)
d_{calc}, g/cm^3	1.461	1.382	1.489
λ, Å	0.71073	0.71073	0.71073
μ, cm^{-1}	0.263	0.209	0.696
T, K	293(2)	293(2)	293(2)
Specimen size, mm	0.50×0.26×0.015	0.60×0.31×0.025	0.35×0.19×0.03
h, *k*, *l* range	$-8 \le h \le 7$, $-15 \le k \le 15$, $-20 \le l \le 20$	$-18 \le h \le 24$, $-4 \le k \le 6$, $-16 \le l \le 19$	$-9 \le h \le 9$, $-9 \le k \le 9$, $-21 \le l \le 34$
Measured/independent reflections	7657/7657	5628/3328, 0.0317	3655/3655
Number of parameters	400	247	254
R_1/wR_2 over N_1	0.0480/0.0722	0.0533/0.0859	0.0571/0.1184
R_1/wR_2 over N_2	0.2239/0.1058	0.1177/0.1063	0.0824/0.1238
S	1.006	0.913	1.039
$\Delta\rho_{(max)}$, $\Delta\rho_{(min)}$, *e*/A^3	0.252, –0.280	0.178, –0.203	0.371, –0.275

amide HL^1, in contrast to the HL^1·DMF solvate (Tables 1 and 2, Figs. 1 and 2). Dihedral angles between mean-square planes of the $S^1N^1N^2N^3C^1C^2$ chains and 5- and 6-membered cycles in HL^1 did not exceed 6.8°, being below 11.1° in the HL^1·DMF molecule. The dihedral angles between 5- and 6-membered cycles in the studied molecules were of 7.1°–10°.

Centrosymmetrical dimers were formed in the structure of HL^1 thioamide due to the N^1–H···S^1 hydrogen bonding. The molecules conformation was stabilized by intramolecular hydrogen bonds (Table 3 and Fig. 3a). The C^{13}–H···O^{2A} hydrogen bonds were formed between the dimers in the crystal as well (Table 3 and Fig. 3b). The π–π-stacking interaction between cycles B ($C^7C^8C^9C^{10}C^{11}C^{12}$) and C ($O^{1A}C^{3A}C^{4A}C^{5A}C^{6A}$) was observed in the structure of HL^1 thioamide as judged from the criterion suggested in [6] (CgI···CgJ < 6.0 Å, β < 60.0°, with β being the angle between the CgICgJ

Table 2. Selected interatomic distances and bond angles in HL^1, HL^1·DMF, and complex **8**

Bond	*d*, Å			Bond	*d*, Å		
	HL^1	HL^1·DMF	complex **8**		HL^1	HL^1·DMF	complex **8**
$Ni^1–N^2$			1.904(3)	$N^3–C^7$	1.400(5)	1.405(3)	1.427(5)
$Ni^1–S^1$			2.1647(12)	$O^3–N^4$	1.226(4)	1.230(3)	1.226(5)
$O^1–C^3$	1.365(4)	1.368(3)	1.389(5)	$C^1–N^1$	1.351(5)	1.366(3)	1.301(5)
$O^4–C^{12}$ (C^{11})	1.366(5)	1.369(3)	1.362(5)	$C^3–C^4$	1.350(5)	1.356(4)	1.352(6)
$O^4–C^{13}$	1.387(5)	1.419(3)	1.416(6)	$C^3–C^2$	1.419(5)	1.429(4)	1.442(6)
$O^2–N^4$	1.216(5)	1.219(3)	1.212(5)	$N^4–C^6$	1.423(6)	1.425(4)	1.428(6)
$N^2–C^2$	1.293(5)	1.283(3)	1.302(5)	$C^6–C^5$	1.336(5)	1.331(4)	1.341(6)
$N^2–N^1$	1.361(4)	1.364(3)	1.383(4)	$C^5–C^4$	1.400(6)	1.412(4)	1.405(6)
$N^3–C^1$	1.331(5)	1.334(3)	1.357(5)				
Angle	ω, deg			Angle	ω, deg		
$N^2Ni^1S^1$			85.13(11)	$O^2–N^4–O^3$	126.2(5)	124.4(3)	125.7(5)
$C^1S^1Ni^1$			96.21(15)	$O^2–N^4–C^6$	118.4(4)	119.1(3)	118.7(4)
$C^2N^2Ni^1$			123.9(3)	$O^3–N^4–C^6$	115.4(4)	116.5(3)	115.6(4)
$N^1N^2Ni^1$			122.2(3)	$C^{11}–C^{12}–O^4$	125.5(4)	125.1(3)	123.1(4)
$C^6O^1C^3$	104.6(3)	104.4(2)	104.5(4)	$C^{11}–C^{12}–C^7$	121.2(4)	120.9(3)	118.9(4)
$C^{12}O^4C^{13}$	118.9(4)	118.1(2)	117.9(4)	$O^4–C^{12}–C^7$	113.3(4)	114.1(3)	
$C^2N^2N^1$	117.6(4)	116.6(2)	113.9(4)	$C^9–C^{10}–C^{11}$	119.8(4)	120.8(3)	119.7(5)
$C^8C^7N^3$	127.7(4)	126.3(3)	117.1(4)	$N^2–C^2–C^3$	120.4(4)	120.4(3)	127.6(4)
$C^8C^7C^{12}$	118.2(4)	119.0(3)	121.6(4)	$C^5–C^6–O^1$	112.7(4)	113.2(3)	113.2(4)
$N^3C^7C^{12}$	114.1(4)	114.8(3)	121.3(4)	$C^5–C^6–N^4$	131.2(5)	131.4(3)	131.2(4)
$N^3C^1N^1$	113.9(4)	113.8(2)	121.3(4)	$O^1–C^6–N^4$	116.1(4)	115.3(3)	115.6(4)
$N^3C^1S^1$	126.5(4)	128.1(2)	115.9(3)	$C^9–C^8–C^7$	120.3(4)	119.6(3)	118.7(5)
$N^1C^1S^1$	119.6(3)	118.1(2)	122.8(3)	$C^6–C^5–C^4$	105.1(4)	105.2(3)	105.2(4)
$C^4C^3O^1$	110.1(4)	110.4(2)	109.7(4)	$C^3–C^4–C^5$	107.5(4)	106.7(3)	107.4(4)
$C^4C^3C^2$	132.1(4)	130.8(3)	138.7(4)	$C^8–C^9–C^{10}$	120.9(5)	120.6(3)	120.9(5)
$O^1C^3C^2$	117.7(4)	118.8(2)	111.5(4)	$C^{12}–C^{11}–C^{10}$	119.6(4)	119.1(3)	120.2(5)
$C^1N^1N^2$	119.5(3)	119.2(2)	111.7(4)				

vector and the normal to the aromatic cycle CgI): the $Cg^1\cdots Cg^2$ distance ($-1+x, y, z$) between the centroids of those fragment equaled 3.57 Å, and the value of β was 15.7°. Besides the marked π–π-interaction, the Y–X···Cg (π-cycle) one was revealed in that compound (X···Cg < 4.0 Å, γ < 30.0°, with γ being the angle between the XCg vector and the normal to the aromatic cycle Cg). For example, the $O^{2A}\cdots$Cg distance for the $N^{4A}–O^{2A}\cdots$B interaction ($C^6C^7C^8C^9C^{10}C^{11}$) (x, y, z) was equal to 3.875 Å, and the γ value equaled 26.2°.

The thioamide and DMF molecules were bound via the $N^2–H\cdots O^4$ and $C^5–H\cdots O^4$ hydrogen bonds in the

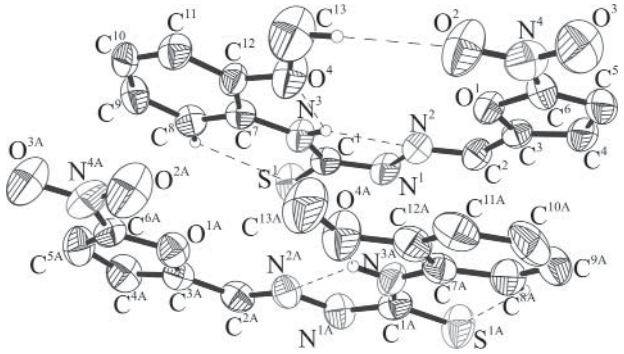

Fig. 1. General view of thioamide HL^1 molecule in the crystal.

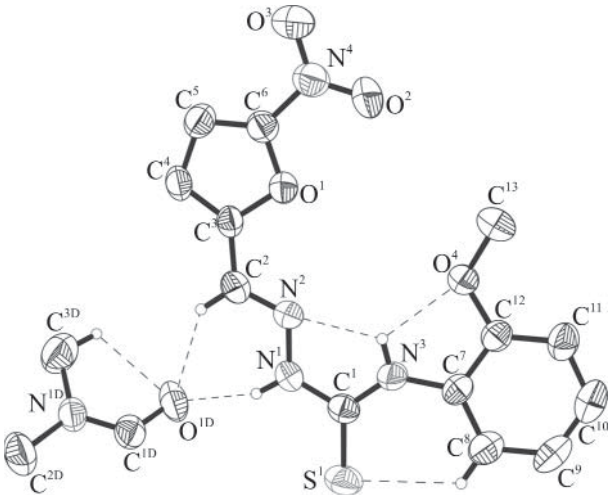

Fig. 2. General view of $HL^1 \cdot DMF$ solvate molecule in the crystal.

$HL^1 \cdot DMF$ solvate, and the van der Waals interaction was revealed between those associates in the crystal (Table 3 and Fig. 4).

The experimental data revealed that the interaction of hot (50–55°C) ethanolic solutions of hydrates of cobalt (nickel, copper) chlorides (nitrates, acetates) with the hydrazine carbothioamides $HL^{1–3}$ (molar ratio 1 : 2) afforded fine-crystalline substances **1**–**18**, their composition being: $M(HL^{1–3})_2X_2$ for complexes **1**–**6**, **10**, **11**, **13**, **14**, **16**, and **17**; $M(L^{1–3})_2$ for complexes **7**–**9**, **12**, **15**, and **18** [M = Co (**1**–**3**), Ni (**4**–**9**), Cu (**10**–**18**); $HL^{1–3} = HL^1$ (**1**, **4**, **7**, **10**–**12**), HL^2 (**2**, **5**, **8**, **13**–**15**), HL^3 (**3**, **6**, **9**, **16**–**18**); X = Cl^- (**1**–**6**, **10**, **13**, **16**), NO_3^- (**11**, **14**, **17**)] as per elemental analysis (Table 4). The obtained coordination compounds **1**–**18** were insoluble in ether, water, and alcohols being readily soluble in DMF, DMSO, and acetonitrile. Yield and physico-chemical parameters of the obtained compounds are listed in Table 4.

Recrystallization of the prepared compounds from DMF gave solvated monocrystals of complex **8**, structure of which was elucidated by means of X-ray diffraction analysis (Fig. 5). The nickel atom was located in the center of symmetry, and the central atom of complex **8** coordinated the S^1 and N^2 atoms of 4-(3-methoxyphenyl)-2-[(5-nitrofuryl)methylene]hydrazine carbothioamide (HL^2) forming the distorted square with distances 2.1647(12) and 1.904(3) Å, respectively. Two planar chelate cycles were this formed, the maximum distortion of the constituting atoms not exceeding 0.13 Å. The dihedral angles between the mean-square planes of the metallocycle A ($Ni^1S^1C^1N^1N^2$) and 5- and 6-membered cycles B ($O^1C^3C^4C^5C^6$) and C ($C^7C^8C^9C^{10}C^{11}C^{12}$) in complex **8** did not exceed 3.19 and 34.84°, respectively.

The molecules of complex **8** in the crystal were bound by DMF molecules owing to the $N^3–H\cdots O^{1D}$, $C^{1D}–H\cdots S^1$, and $C^{12A}–H\cdots O^3$ hydrogen bonds,

(a) (b)

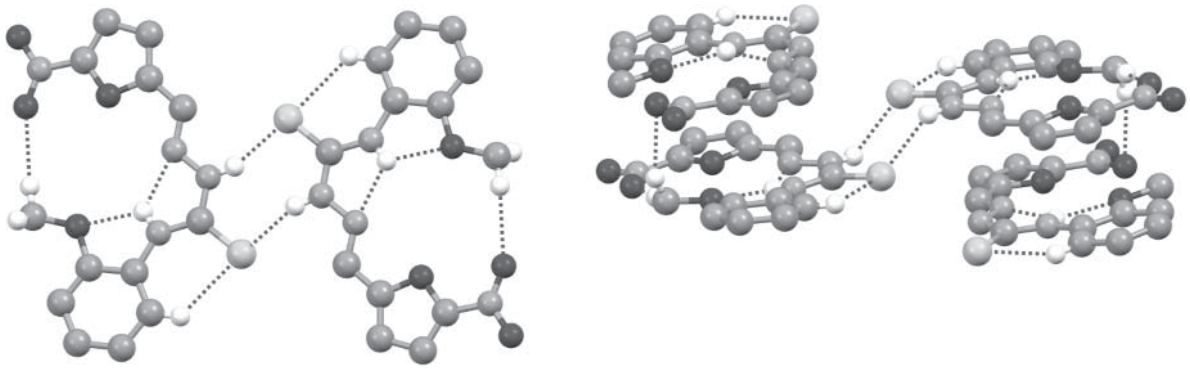

Fig. 3. Fragments of thioamide HL1 packing: (a) formation of dimers and (b) hydrogen bond between the dimers.

Table 3. Geometry parameters of hydrogen bonds in HL^1, HL^1·DMF, and complex **8**

D–H···A bond	Distance, Å			DHA angle, deg	Coordinates of atom A
	D–H	H···A	D···A		
N^1–H^1···S^1					
N^3–H^3···O^4	0.86	2.05	2.5195	1114	*x*, *y*, *z*
N^3–H^3···N^2	0.86	2.09	2.5601	114	*x*, *y*, *z*
N^{3A}–H^{3A}···O^{4A}	0.86	2.07	2.5361	113	*x*, *y*, *z*
N^{3A}–H^{3A}···N^{2A}	0.86	2.11	2.5740	113	*x*, *y*, *z*
C^8–H^8···S^1	0.93	2.62	3.2702	127	*x*, *y*, *z*
C^{8A}–H^{8A}···S^{1A}	0.93	2.62	3.2702	127	*x*, *y*, *z*
C^{13}–H^{13E}···O^{2A}	0.96	2.60	3.5030	157	–1 + *x*, *y*, *z*
C^{13}–H^{13F}···O^2	0.96	2.55	3.5045	177	*x*, *y*, *z*
HL^1·DMF					
N^1–H^1···O^{1D}					
N^3–H^3···O^4	0.86	2.11	2.5499	111	*x*, *y*, *z*
N^3–H^3···N^2	0.86	2.10	2.5687	114	*x*, *y*, *z*
C^2–H^2···O^{1D}	0.93	2042	3.2069	142	*x*, *y*, *z*
C^{3D}–H^{3DC}···O^{1D}	0.96	2.35	2.7643	106	*x*, *y*, *z*
C^8–H^8···S^1	0.93	2.63	3.2669	126	*x*, *y*, *z*
Complex **8**					
N^3–H^3···O^{1D}					
C^{1D}–H^{1D}···S^1	0.93	2.78	3.5057	136	*x*, –1+ *y*, *z*
C^2–H^2···S^1	0.93	2.41	3.0324	124	–*x*, 1 – *y*, -*z*
C^4–H^4···N^1	0.93	2.56	2.9272	104	*x*, *y*, *z*
C^5–H^5···O^4	0.93	2.39	3.2398	152	–*x*, –1/2 + *y*, 1/2 – *z*
C^{12A}–H^{3DB}···O^3	0.96	2.59	3.3908	141	1+ *x*, 1+ *y*, *z*
C^{3D}–H^{3DC}···O^{1D}	0.96	2.39	2.7426	101	*x*, *y*, *z*
C^{12}–H^{12}···N^1	0.93	2.49	2.9436	110	*x*, *y*, *z*

forming the chains. The chains were united via the C^5–H···O^4 hydrogen bonds (Table 3 and Fig. 6). As judged from the criterion suggested in Ref. [6], the Y–X···Cg (π-cycle) interaction was observed in the structure of compound **8** (X···Cg < 4.0 Å, γ < 30.0°, γ being the angle between the XCg vector and the normal to the aromatic cycle Cg). For example, the X···Cg distances for the N^4–O^2···A (*x*, –1+*y*, *z*) and N^4–O^3···A (–*x*, –*y*, –*z*)interactions were 3.56, 3.77 Å, respectively, and the γ values equaled 19.49 and 22.85°. Besides the marked Y–X···π interaction, the Y–H···Cg (π-cycle) interaction was observed in the molecule of compound **8** (H···Cg < 3.0 Å, γ < 30.0°, γ being the angle between the HCg vector and the normal to the aromatic cycle Cg). The H···Cg distances for the C^{13}–H···C (–*x*, –1/2+*y*, 1/2–*z*) and C^{2D}–H···A (*x*, *y*, *z*) interactions were 2.79 and 2.87 Å, respectively, the values of γ being 4.73° and 17.22°.

Table 4. Physico-chemical parameters of coordination compounds **1**–**18**

Compound no.	Yield, %	μ_{eff}[a], μ_B	æ[a], Ω^{-1} cm^2 mol^{-1}	Found, %				Formula	Calculated, %			
				M	N	S	Cl		M	N	S	Cl
1	77	4.85	3	7.37	14.30	8.00	8.98	$C_{26}H_{24}Cl_2CoN_8O_8S_2$	7.65	14.55	8.32	9.21
2	76	4.80	3	7.44	14.25	8.09	9.12	$C_{26}H_{24}Cl_2CoN_8O_8S_2$	7.65	14.55	8.32	9.21
3	70	4.91	4	7.40	14.37	8.04	8.95	$C_{26}H_{24}Cl_2CoN_8O_8S_2$	7.65	14.55	8.32	9.21
4	75	2.98	4	7.41	14.31	8.11	9.01	$C_{26}H_{24}Cl_2N_8NiO_8S_2$	7.62	14.55	8.32	9.22
5	86	2.90	3	7.50	14.62	8.07	9.01	$C_{26}H_{24}Cl_2N_8NiO_8S_2$	7.62	14.55	8.32	9.22
6	80	3.09	2	7.87	14.39	8.11	8.97	$C_{26}H_{24}Cl_2N_8NiO_8S_2$	7.62	14.55	8.32	9.22
7	77	[b]	2	8.12	15.80	8.97	–	$C_{26}H_{22}N_8NiO_8S_2$	8.42	16.07	9.20	–
8	75	[b]	2	8.17	15.92	9.00	–	$C_{26}H_{22}N_8NiO_8S_2$	8.42	16.07	9.20	–
9	63	[b]	3	8.25	16.01	8.91	–	$C_{26}H_{22}N_8NiO_8S_2$	8.42	16.07	9.20	–
10	70	1.91	4	8.01	14.55	7.98	8.89	$C_{26}H_{24}Cl_2CuN_8O_8S_2$	8.20	14.46	8.27	9.16
11	71	2.15	5	7.50	16.77	7.85	–	$C_{26}H_{24}CuN_{10}O_{14}S_2$	7.67	16.92	7.74	–
12	79	1.80	2	8.87	16.09	8.85	–	$C_{26}H_{22}CuN_8O_8S_2$	9.05	15.96	9.13	–
13	74	1.88	3	7.91	14.19	8.01	8.97	$C_{26}H_{24}Cl_2CuN_8O_8S_2$	8.20	14.46	8.27	9.16
14	60	1.97	5	7.48	17.07	7.48	–	$C_{26}H_{24}CuN_{10}O_{14}S_2$	7.67	16.92	7.74	–
15	75	2.08	2	8.75	15.71	8.85	–	$C_{26}H_{22}CuN_8O_8S_2$	9.05	15.96	9.13	–
16	72	1.90	4	7.93	14.17	8.03	9.00	$C_{26}H_{24}Cl_2CuN_8O_8S_2$	8.20	14.46	8.27	9.16
17	61	1.87	5	7.42	16.70	7.65	–	$C_{26}H_{24}CuN_{10}O_{14}S_2$	7.67	16.92	7.74	–
18	76	2.02	2	8.78	15.67	8.85	–	$C_{26}H_{22}CuN_8O_8S_2$	9.05	15.96	9.13	–

[a] At 292 K. [b] The complex is diamagnetic.

Purity and structure of other complexes were elucidated using the data on elemental analysis, molecular electroconductivity, magnetochemistry, and IR spectroscopy. The determined molar electroconductivity (æ) of the prepared compounds in DMF revealed that they were non-electrolytes (æ = 2–5 Ω^{-1} cm^2 mol^{-1}).

Magnetochemical study of complexes **1**–**18** at room temperature (292 K) revealed that cobalt and nickel complexes **4**–**6** were paramagnetic (Table 4) and, basing on their magnetochemical properties, their central atoms were in the pseudo octahedral ligand surrounding (electronic state $t^5{}_{2g}e^2{}_g$ and $t^6{}_{2g}e^2{}_g$, respectively). Other nickel compounds **7**–**9** were diamagnetic and likely square-planar. The effective magnetic moments of the copper compounds corresponded to the spin values of a single unpaired electron. Those experimental data suggested the monomeric structure of the complexes.

To elucidate the details of the ligands coordination with the central atom, we compared the IR spectra of the prepared complexes **1**–**18**, starting azomethines $HL^{1–3}$, and coordination compound **8** with the structure known from the X-ray diffraction analysis. It was found that the thioamides $HL^{1–3}$ acted as bidentate N,S-ligands, being attached to the complex forming ion via the azomethine nitrogen and the sulfur atoms, giving the five-membered metallocycle. That was evidenced by shift of the ν(C=N) and ν(C=S) absorption bands (observed in the spectra of the starting thioamides $HL^{1–3}$ at 1610–1590 and

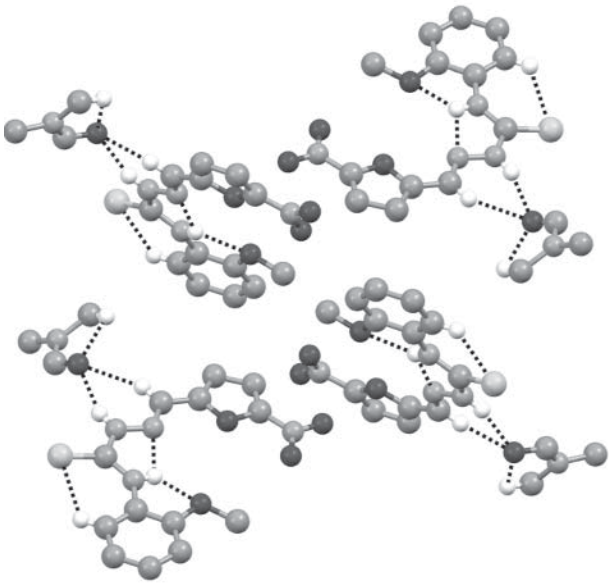

Fig. 4. Fragment of crystal packing of the HL^1·DMF solvate.

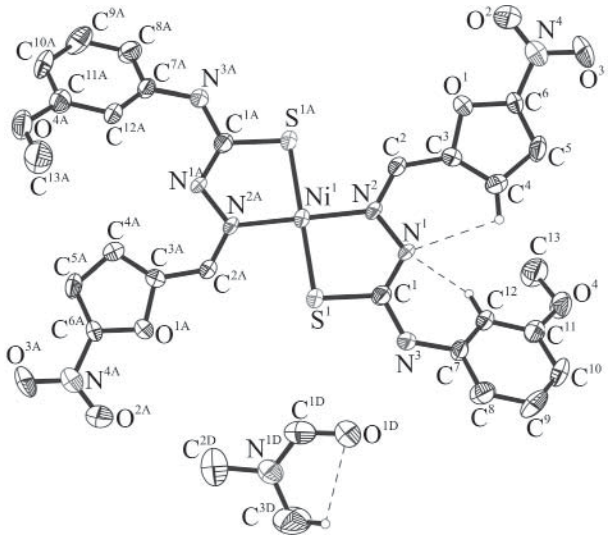

Fig. 5. General view of complex **8** solvate in the crystal.

780–770 cm^{-1}, respectively) by 25–15 cm^{-1}. Participation of sulfur of the $HL^{1–3}$ ligands protonated thienol form in the coordination with central ions was confirmed by the disappearance of the ν(C=S) (780–770 cm^{-1}) and ν(NH) (3210–3200 and 3170–3150 cm^{-1}) absorption bands in the IR spectra of complexes **7–9**, **12**, **15**, and **18** and the appearance of a new band at 605–585 cm^{-1} assignable to the ν(C–S) vibration according to the reference data [7]. Furthermore, the IR spectra of those compounds contained absorption bands at 1570–1560 cm^{-1}, assignable to the >C=N–N=C< stretching [8–10]. The above-mentioned coordination of the $HL^{1–3}$ thioamides was also confirmed by the appearance of a series of absorption bands at 530–405 cm^{-1}, assigned to the ν(M–N) (525–505 and 430–405 cm^{-1}) and ν(M–S) (450–440 cm^{-1}) vibrations. Participation of other functional groups of the $HL^{1–3}$ thioamides in the coordination with the central ion was ruled out, since their characteristic absorptions were not changed in comparison with the starting thioamides.

The obtained physico-chemical data allowed representation of chemical bonding in complexes **1–18** as structures **A** and **B** (Scheme 2).

It has been found that many complexes of bioactive metals with thiosemicarbazones of aldehydes and ketones can selectively suppress the growth and propagation of various microorganisms [11–13]. In view of that, we performed *in vitro* studies of antimicrobial and antifungal activity of the prepared compounds **1–18** towards a series of standard strains of *Staphylococcus aureus*, coliform

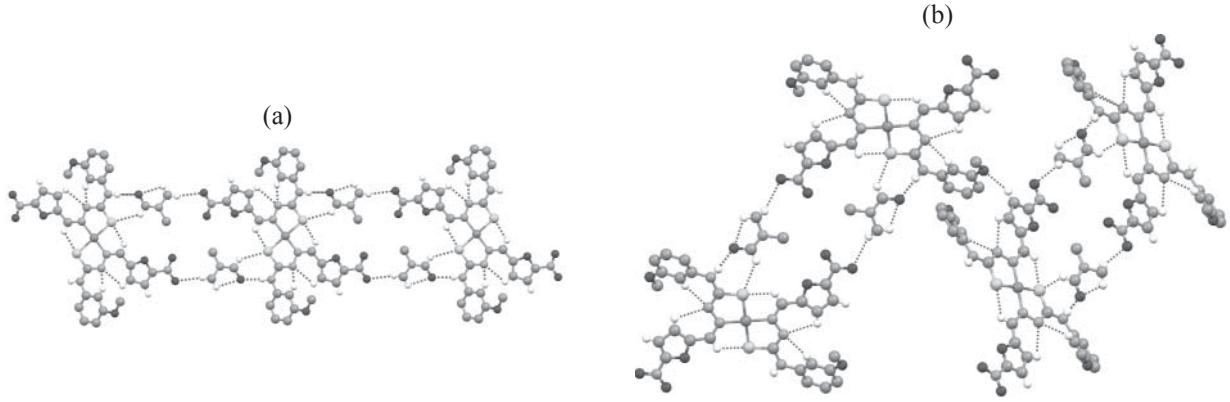

Fig. 6. Fragments of crystal packing of complex **8**: (a) formation of the chains in the crystal, (b) formation of hydrogen bond between the chains.

Scheme 2.

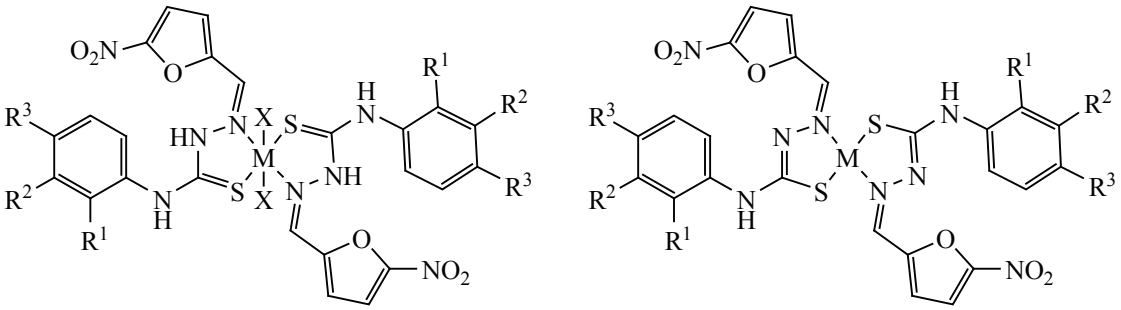

A **B**

A: M = Co, Ni, Cu; X = Cl^-, NO_3^-; R^1 = H, CH_3; R^2 = H, CH_3; R^3 = H, CH_3. **B**: M = Ni, Cu; R^1 = H, CH_3; R^2 = H, CH_3; R^3 = H, CH_3.

bacillus (*Escherichia coli* and *Klebsiella pneumoniae*), and yeast-like fungi (*Candida albicans*). The obtained experimental data (Table 5) revealed that the starting cobalt, nickel, and copper salts as well as thioamides $HL^{1–3}$ did not exhibit antimicrobial activity against the listed microorganisms, whereas complexes **1–18** exhibited selective bacteriostatic and bactericide activity at concentration of 0.03–1.0 mg/mL (against staphylococcus and fungi) and 0.5–1.0 mg/mL (against coliform bacillus). The experiment revealed that the minimal inhibitory concentration (MIC) and minimal bactericide concentration (MBC) of the studied complexes were strongly affected by the nature of the central atom and the acido ligand as well as by the methoxy group position in azomethines $HL^{1–3}$. Other factors being the same, the complexes activity followed the series: Cu ≥ Co > Ni, $Cl^- \geq NO_3^-$, and $HL^1 > HL^2 \geq HL^3$. Moreover, the closeness of the MIC and MBC values for many compounds evidenced their bactericide action. The discussed experimental data revealed the prospects of further development of antimicrobial and antifungal coordination compounds of bioactive metals with hydrazine thioamide ligands.

EXPERIMENTAL

X-ray diffraction analysis was performed using a Gemini diffractometer (Oxford Diffraction) [14]. The structures were used via direct method and refined via least squares method under anisotropic approximation for non-hydrogen atoms using SHELX-97 software [15]. Hydrogen atoms were included into the refinement in the geometrically calculated positions, and their temperature factors U_H were taken 1.2 times higher than those of the adjacent carbon and oxygen atoms. Coordinates of the basis atoms were deposited at the Cambridge Crystallographic Data Centre (CCDC 1536619, 1536620, 1536621). Geometry calculations and plotting were performed using PLATON [16] and Mercury [15], respectively, the packing was presented omitting hydrogen atoms not involved in the hydrogen bonding.

Resistance of the solutions of complexes **1**–**18** in DMF (20°C, c = 0.001 mol/L) was measured using an R-38 rheochord bridge. IR spectra were recorded using an ALPHA spectrometer (4000–400 cm^{-1}). Effective magnetic moment was determined via the Gouy method. Molar magnetic susceptibility was calculated accounting for diamagnetism basing on the theoretical values of magnetic susceptibility of organic compounds.

Starting *N*-(2-methoxyphenyl)- (mp 163–165°C), *N*-(3-methoxyphenyl)- (mp 175–177°C), and *N*-(4-methoxyphenyl)hydrazine carbothioamide (mp 156–158°C) were prepared as described elsewhere [17]. Antimicrobial and antifungal activity were tested *in vitro* via double dilution in a liquid medium (meat infusion broth, pH = 7.0) following the standard protocol [18].

***N*-(2-Methoxyphenyl)-2-[(5-nitrofuryl)methylene]-hydrazine carbothioamide (HL^1).** A hot (55–60°C) solution of 10 mmol of 5-nitrofuran-2-carbaldehyde in 15 mL of ethanol was mixed with a solution of 10 mmol of *N*-(2-methoxyphenyl)hydrazine carbothioamide in 35 mL of ethanol. Light yellow precipitate formed upon cooling was filtered off, washed with small amount of ethanol, and dried in air. Yield 71%, mp 230–232°C. Found, %: C 48.60; H 3.77; N 17.35; S 9.87. $C_{13}H_{12}N_4O_4S$. Calculated, %: C 48.75; H 3.78; N 17.49; S 10.01.

Compounds HL^2 and HL^3 were prepared similarly from 5-nitrofuran-2-carbaldehyde and *N*-(3-methoxyphenyl)hydrazine carbothioamide (in the case of HL^2)

or *N*-(4-methoxyphenyl)hydrazine carbothioamide (in the case of HL^3) in the 1 : 1 molar ratio.

Compound HL^2. Yield 65%, mp 201–203°C. Found, %: C 48.51; H 3.60; N 17.30; S 9.81. $C_{13}H_{12}N_4O_4S$. Calculated, %: C 48.75; H 3.78; N 17.49; S 10.01.

Compound HL^3. Yield 70%, mp 213–215°C. Found, %: C 48.67; H 3.68; N 17.29; S 9.80. $C_{13}H_{12}N_4O_4S$. Calculated, %: C 48.75; H 3.78; N 17.49; S 10.01.

Thioamides $HL^{1–3}$ were readily soluble in DMF and DMSO as well as in alcohols (at heating).

Dichlorobis{*N*-(2-methoxyphenyl)-2-[(5-nitro-furyl)methylene]hydrzxine carbothioamido}cobalt (1). A solution of 10 mmol of cobalt(II) chloride hexahydrate in 20 mL of ethanol was added to a solution of 20 mmol of *N*-(2-methoxyphenyl)-2-[(5-nitrofuryl)methylene]-hydrazine carbothioamide (HL^1) in 30 mL of ethanol at stirring and heating (50–55°C). The reaction mixture was refluxed during 50–60 min, cooled to ambient, and slowly evaporated. Dark brown precipitate was filtered off, washed with small amount of ethanol, and dried in air to constant mass.

Complexes **2**–**18** were prepared similarly.

CONFLICT OF INTERESTS

No conflict of interests was declared by the authors.

REFERENCES

1. Mashkovskii, M.D., *Lekarstvennye sredstva* (Drugs), Moscow: Novaya Volna, 2012.
2. Kalinowski, D.S. and Richardson, D.R., *Pharmacol. Rev*., 2005, vol. 57, no. 4, p. 547. doi 10.1124/pr.57.4.2
3. Beraldo, H. and Gambino, D., *Mini-Rev. Med. Chem*., 2004, vol. 4, no. 1, p. 31. doi 10.2174/ 1389557043487484
4. Ulkuseven, B., Bal-Demirci, T., Akkurt, M., Yalcin, S.P., and Buyukgungor, O., *Polyhedron*, 2008, vol. 27, p. 3646. doi 10.1016/j.poly.2008.08.024
5. Gulea, A.P., Lozan-Tyrshu, K.S., Tapcov, V.I., Korzha, I.D., and Rudik, V.F., *Russ. J. Gen. Chem*., 2012, vol. 82, no. 11, p. 1869. doi 10.1134/S1070363212110242
6. Spek, A.L., *J. Appl. Cryst*., 2003, vol. 36, p. 7. doi 10.1107/S0021889802022112
7. Nakamoto, K., Infrared *Spectra of Inorganic and Coordination Compounds*, New York: Wiley Interscience, 1963.
8. Gulea, A.P., Spynu, S.N., Tsapkov, V.I., and Poirier, D., *Russ. J. Gen. Chem*., 2008, vol. 78, no. 8, p. 984. doi 10.1134/S1070363208050253
9. Gulea, A.P., Prisacari, V.I. , Tsapkov, V.I., Buracheva, S.A., Spynu1, S.N., Bezhenari, N.P., Poirier, D., and Roy, J., *Pharm. Chem. J*., 2007, vol. 41, no. 11, p. 596. doi 10.30906/0023-1134-2007-41-11-29-32
10. Gulea, A.P., Prisacari, V.I., Tsapkov, V.I., Buracheva, S.A., Spynu, S.N., and Bezhenari, N.P., *Pharm. Chem. J*., 2008, vol. 42, no. 11, p. 326. doi 10.30906/0023-1134-2008-42-6-19-21
11. Pahontu, E., Fala, V., Gulea, A., Poirier, D., Tsapkov, V., and Rosu, T., *Molecules*, 2013, no. 18, p. 8812. doi 10.3390/molecules18088812
12. Pahontu, E., Julea, F., Rosu, T., Purcarea, V., Chumakov, Yu., Petrenko, P., and Gulea, A., *J. Cell. Mol. Med*., 2015, vol. 19, no. 4, p. 865. doi 10.1111/jcmm.12508
13. Pathan, A.H., Bakale, R.P., Naik, G.N., Frampton, C.S., and Gudasi, K.B., *Polyhedron*, 2012, vol. 34, no. 1, p. 149. doi 10.1016/j.poly.2011.12.033
14. *CrysAlisPro*, Version 1.171.33.52 (release 06-11-2009 CrysAlis171.NET). Oxford Diffraction Ltd.
15. Sheldrich, G.M., *Acta Cryst. (A)*, 2008, vol. 64, p. 112. doi 10.1107/S0108767307043930
16. Macrae, C.F., Edgington, P.R., McCabe, P., Pidcock, E., Shields, G.P., Taylor, R., Towler, M., and Van De Streek, J., *J. Appl. Cryst*., 2006, vol. 39, p. 453. doi 10.1107/S002188980600731X
17. Saswati, Dinda, R., Schmiesing, C., Sinn, E., Patil, Y.P., Nethaji, M., Stoeckli-Evans, H., and Acharyya, R., *Polyhedron*, 2013, vol. 50, p. 354. doi 10.1016/j.poly.2012.11.031
18. Gulea, A., Poirier, D., Roy, J., Stavila, V., Bulimestru, I., Tapcov, V., Birca, M., and Popovschi, L., *J. Enzyme Inhib. Med. Chem*., 2008, vol. 23, no. 6, p. 806. doi 101080/14756360701744300 2